



## Calibrating estimates of ionospheric long-term change

Christopher Scott<sup>1,2</sup>, Matthew Wild<sup>2</sup>, Luke Barnard<sup>1</sup>, Bingkun Yu<sup>3</sup>, Tatsuhiro Yokoyama<sup>5</sup>,  
Michael Lockwood<sup>1</sup>, Cathryn Mitchel<sup>4</sup>, John Coxon<sup>6</sup>, and Andrew Kavanagh<sup>7</sup>

<sup>1</sup>Department of Meteorology, University of Reading, Berkshire, RG6 6BB, UK

<sup>2</sup>RAL Space, Rutherford Appleton Laboratory, Chilton, Oxfordshire, OX11 0QX, UK

<sup>3</sup>Institute of Deep Space Sciences, Deep Space Exploration Laboratory, Hefei, 230088, China

<sup>4</sup>Department of Electronic Electrical Engineering, University of Bath, BA2 7AY, UK

<sup>5</sup>Research Institute for Sustainable Humanosphere, Kyoto University, Uji, Kyoto 611-0011, Japan

<sup>6</sup>Department of Mathematics, Physics and Electrical Engineering, Northumbria University, UK.

<sup>7</sup>British Antarctic Survey, High Cross, Madingley Road, Cambridge, CB3 0ET, UK

**Correspondence:** Christopher Scott (chris.scott@reading.ac.uk)

**Abstract.** Long-term change in the height of the ionospheric F2 layer,  $hmF2$ , is predicted to result from increased levels of tropospheric greenhouse gases. Sufficiently long sequences of ionospheric data exist to investigate this long-term change, recorded by a global network of ionosondes. However, direct measurements of ionospheric layer height with these instruments is not possible. As a result, most estimates of  $hmF2$  rely on empirical formulae based on parameters routinely scaled from ionograms. Estimates of trends in  $hmF2$  using these formulae show no global consensus. We present an analysis in which data from the Japanese ionosonde station at Kokubunji were used to estimate monthly median values of  $hmF2$  using an empirical formula. These were then compared with direct measurements of the F2 layer height determined from Incoherent Scatter measurements made at the Shigaraki MU observatory, Japan. Our results reveal that the formula introduces diurnal, seasonal and long-term biases in the estimates of  $hmF2$  of  $\approx \pm 10\%$  ( $\pm 25km$  at an altitude of  $250km$ ). These can be explained by the presence of underlying F1 layer ionisation not accounted for in the formula. We demonstrate, that for Kokubunji, the ratio of F2/F1 peak electron concentrations is strongly controlled by changes in geomagnetic activity represented by the  $am$  index. Changes in thermospheric composition in response to geomagnetic activity have been shown to be highly localised. We conclude that localised changes in thermospheric composition modulate the F2/F1 peak ratio, leading to differences in  $hmF2$  trends. We further conclude that the influence of thermospheric composition on the underlying ionosphere needs to be accounted for in these empirical formulae if they are to be applied to studies of long-term ionospheric change.

### 1 Introduction

The concept of long-term change in the upper atmosphere and ionosphere due to anthropogenic production of  $CO_2$  and  $CH_4$  (popularly called the 'greenhouse effect') was first considered by Roble and Dickinson (1989). Using a coupled mesosphere, thermosphere and ionosphere model, they concluded that the thermosphere would be expected to cool by around 50K as a result of a doubling of the  $CO_2$  and  $CH_4$  in the lower atmosphere, thereby trapping more heat in the troposphere. Rishbeth (1990) examined the consequences of such a cooling on the ionosphere and concluded that the height of the ionospheric F2

peak,  $hmF2$ , would be reduced by around 20 km as a result, though changes to the peak density of the F2 layer,  $f_oF2$ , would be small.

Despite the existence of long-term ionospheric data sets, extracting this signal is challenging. In addition to any contraction  
25 of the thermosphere due to greenhouse forcing, there are other mechanisms that will change the height of the ionosphere, on a range of timescales.

The behaviour of the upper atmosphere is largely controlled by variations in solar activity, both through changes in ionising solar radiation and through interaction of the solar wind (in the form of fast solar wind streams and coronal mass ejections, CMEs) with the Earth's magnetosphere which influences the ionosphere and thermosphere by driving currents that cause  
30 heating. Changes in solar ionising radiation follow the eleven-year activity cycle, with more Extreme Ultra-Violet (EUV) and X-ray radiation incident on the Earth's upper atmosphere at solar maximum, leading to greater plasma production in the ionosphere (see e.g. Rishbeth (1988)). Superimposed on this trend are transient enhancements due to solar flare activity. The solar wind consists of a magnetised plasma flowing supersonically from the Sun and filling interplanetary space. Here, the magnetic field becomes known as the Heliospheric Magnetic Field (HMF). The constant outflow contains fast ( $\sim 750\text{km s}^{-1}$ )  
35 and slow ( $\sim 400\text{km s}^{-1}$ ) streams, with transient CMEs producing localised regions of modulated solar wind density, speed and magnetic field for periods of a few days. If the HMF and geomagnetic fields are oppositely aligned, the two fields can 'reconnect', (Dungey, 1961) enhancing the flow of energetic particles into the upper atmosphere at high latitudes, and increasing electric fields, both of which cause localised heating (e.g. McCrea et al. (1991)). The resulting expansion of the thermosphere brings molecular-rich neutral gasses to higher altitudes where it enhances the loss rate of ionisation, causing a depletion of the  
40 ionosphere (King, 1963). This molecular-rich air is subsequently transported equatorward by general circulation, extending the influence of the geomagnetic activity globally, with the magnitude of the response decreasing with decreasing geomagnetic latitude (e.g. Rishbeth et al. (1985)). While this is a necessarily brief summary of solar-terrestrial interactions, a detailed review of the subject is given by Pulkkinen (2007) and Schwenn (2006).

Above a given ionospheric monitoring station therefore, changes to the height of the ionosphere are a superposition of several  
45 different effects;

1. Geomagnetic activity causes heating of the thermosphere which increases the height of ionospheric layers, which tend to lie at constant pressure levels.
2. Solar irradiance modulates the energy input to the atmosphere, increasing the electron production and changing the height of the ionospheric layers due to the thermal expansion of the atmosphere.
- 50 3. Changes in thermospheric composition alter the shape of the ionisation profile, with such changes becoming apparent on an ionogram through the visibility of the F1 layer and a weakening of the F2 peak due to molecular species enhancing the loss rate of ionisation at greater altitudes.
4. At the higher altitudes of the F2 layer, the relatively long lifetime of individual ions and electrons means that they can be transported through collision with the neutral winds. Therefore changes to the wind pattern influence the height of the F2 layer,  
55 with poleward winds blowing ionisation down the field-lines to lower altitudes and equatorward winds blowing ionisation up the field-lines to higher altitudes.



5. Of a smaller magnitude, there are influences from the lower atmosphere, including contraction of the thermosphere due to the presence of enhanced quantities of greenhouse gasses in the lower atmosphere.

60 Since long-term sequences of data exist from the global network of ionospheric monitoring stations, covering an epoch of more than 90 years, many studies have attempted to detect the predicted contraction of the ionosphere in response to enhanced greenhouse gasses. One popular technique is to fit proxies for geomagnetic activity and solar irradiance to the data. Variations in F2 layer height introduced by (1) and (2) are accounted for by subtracting the fit from the data, with any residual long-term drift due to the contraction of the thermosphere assumed to be the dominant part of (4) and (5). When such a technique is applied globally, no consistent pattern has yet emerged from a global analysis of these data (e.g. Bremer et al. (2004)) which  
65 has been attributed (e.g. Jarvis et al. (1998), Bremer (1998)) to phenomena that are unaccounted for in the analysis such as localised changes to thermospheric circulation (4).

### 1.1 Measuring the ionosphere using ground-based radar

Free electrons in the Earth's ionosphere resonate at a frequency related to the local electron concentration such that  $f = 8.98\sqrt{N}$  where  $f$  is the frequency in  $Hz$  (known as the plasma frequency) and  $N$  is the electron concentration in  $m^{-3}$ . For  
70 the plasma concentrations present in the Earth's ionosphere, this relates to frequencies in the High Frequency (HF) range of the radio spectrum, typically between  $1 - 20MHz$ . A radio signal (of the so-called 'ordinary wave' with left-handed circular polarisation, see Rishbeth and Garriott (1969)) launched vertically will be returned from the ionosphere when it reaches an altitude at which the radio frequency matches the local plasma frequency. By transmitting a series of ordinary wave radio pulses across a range of frequencies and measuring the time for each to be returned from the ionosphere, a vertical profile of  
75 the ionospheric electron concentration can be obtained. Data from a such a sounding is usually presented as a plot of time-of-flight against radio frequency known as an ionogram. By assuming the pulse is travelling at the speed of light in a vacuum, the time-of-flight can be converted to a height in  $km$ , though since the presence of plasma delays the pulse, these heights become exaggerated and are known as 'virtual' heights,  $h'$ . The virtual height of the F2 layer, for example would be expressed as  $h'F2$ . In contrast, the peak frequency returned from each layer is an absolute value, denoted by  $f_o$ , so, for example, the peaks of  
80 the E and F2 layers would be represented as foE and foF2 respectively. The 'o' represents the 'ordinary' ray path since the presence of the Earth's magnetic field makes the ionosphere birefringent, creating an alternative 'extraordinary' ray path for radio pulses propagating with the opposite polarisation. It is possible to 'invert' an ionogram to obtain the true height profile by integrating along the virtual height profile, accounting for the presence of ionisation at each height step, with assumptions made about the ionisation within the unobserved 'valley' between the E and F regions (e.g. Rishbeth and Garriott (1969)). This  
85 process was time-consuming and so was not carried out routinely in the early days of ionospheric research. With the advent of digital sounders and the ability to automatically identify and invert ionograms, true-height analysis is now far more readily available but, alas, does not yet cover sufficiently long time intervals to allow meaningful estimates of trends in ionospheric layer heights. When derived, the true height of each layer is denoted by  $hm$  such that the true height of the F2 layer peak is  $hmF2$ .



## 90 1.2 Using ionosonde data to estimate $hmF2$

Temperature trends in troposphere and stratosphere have been defined by re-analysis of data, for example from the GNSS RO, ERA5, MERRA2, and ERA-I satellites citepshangguan2019. These authors show that tropospheric warming is accompanied by stratospheric cooling - a unique signature of the greenhouse gas effect. However, this can only be observed for the interval of regular global stratospheric temperature data. Shangguan et al. (2019) studied the interval 2002-2017 and this was recently extended to 1986-2022 by Santer et al. (2023). The trend is also detected in balloon radiosonde data extending back to 1978 citephilipona2018 but these data also show that the trend slowed, stopped or even reversed, depending in location, around 2000 because of the recovery of the ozone layer. In comparing these studies it is important to remember that these effects are altitude dependent which will lead to differing results. Searching for a descent in ionospheric layers is valuable because it would be the integrated effect of upper atmosphere cooling over all altitudes. The longevity of ionospheric data series offers the potential to extend observations of stratospheric cooling back by a further five decades, provided the cooling effect trend can be extracted from the data, allowing for all other effects.

The first published analysis (Bremer, 1992) of long-term trends in  $hmF2$  was for the mid-latitude station at Juliusruh ( $54.6^{\circ}N$ ,  $13.4^{\circ}E$ ) and provided evidence for a decrease of the peak height of the ionospheric F2-layer. The associated long-term variations of the peak electron concentration were small, consistent with the modelling work by Rishbeth (1990). Subsequent work (Bremer, 1998) repeated the analysis for 31 stations in the European sector for which long-term ionospheric records exist. Bremer concluded that in the F2 region, there was no consistent trend, with stations west of  $30^{\circ}E$  showing negative trends in  $hmF2$  and peak electron concentration (inferred from  $foF2$ ) whereas positive trends in both parameters dominated in data from stations to the east of  $30^{\circ}E$ . Bremer further remarked that these longitudinal differences probably resulted from dynamical effects in the F2 layer.

Jarvis et al. (1998) presented an analysis of long-term trends in  $hmF2$  observed in two Southern-Hemisphere stations. They reported long-term changes in altitude, which showed seasonal and diurnal variation, at both sites. The magnitude of the long-term trend was altitude-dependent which, they argued, could be interpreted either as a constant decrease in altitude combined with a decreasing thermospheric wind effect or as a constant decrease in altitude which is altitude-dependent.

Of particular relevance to the current paper is the work of Xu et al. (2004) who conducted an analysis of data from the ionosonde station at Kokubunji in Japan with monthly medians of ionosonde observations taken over a period of more than four solar cycles. Using a linear regression model to eliminate solar and geomagnetic effects, they determined a decreasing trend in  $hmF2$  of  $0.398km/year$  at noon and  $0.505km/year$  at midnight. In addition, they analysed seasonal and diurnal trend variations. They found that the seasonal variations of  $hmF2$  at noon and midnight were opposite to each other, though the long-term trends at both times remained negative. The data indicated that the effect of geomagnetic activity was not significant in regression models applied to data recorded at this station.

Bremer et al. (2004) presented an analysis of global trends in a number of ionospheric parameters, including  $hmF2$ . They concluded that, in the F2 layer, the scatter of trends for the different stations was high and no significant mean global trends could be estimated.



There have subsequently been many studies made of  $hmF2$  trends, the summarisation of which lies beyond the scope of  
125 this paper. A useful review of more recent investigations into long-term ionospheric trends has been presented by Lastovicka  
(2013).

While details of the analysis technique differ between studies, long-term trends in  $hmF2$  are usually determined in the fol-  
lowing way. 1. An empirical formula based on standard ionosonde scaled parameters (usually monthly medians of  $f_oF2$ ,  $f_oE$   
and  $M3000F2$ ) is used to estimate  $hmF2$  over an extended time period (preferably several decades). 2. Having determined  
130 the long-term trend in  $hmF2$ , the influence of variability in geomagnetic activity and solar irradiance is estimated by fitting  
proxies for these (usually the  $A_p$  index and solar  $f_{10.7cm}$  flux respectively) to the  $hmF2$  data. 3. This two parameter fit is  
then subtracted from the original data and any difference is considered to be due to local environmental change, such as via  
greenhouse forcing.

Mikhailov and Marin (2001) argued that the observed  $F2$  trends were strongly dependent on the long-term variations in  
135 geomagnetic activity through changes in composition of the neutral thermosphere, thermospheric temperature and changes  
to the neutral wind. They subdivided the time-series to demonstrate that the observed trend in  $F2$  parameters was dependent  
on the rate of change in the geomagnetic activity. Subsequent work (Mikhailov, 2006) proposed that the difference in  $hmF2$   
trends seen across Europe could be explained by differences in thermospheric winds.

Scott et al. (2014) presented long-term changes in the relative strength of the annual and semiannual variability in the  
140  $f_oF2$  critical frequencies at Slough/Chilton in the UK which were highly anticorrelated with those recorded at Stanley in the  
Falkland Islands. The dominance of annual or semi-annual variations in  $f_oF2$  is a function of thermospheric composition and  
so they argued that the observed long-term changes are due to changes in thermospheric composition driven by geomagnetic  
activity. Since the response was so different at the two stations, Scott et al. (2014) also suggested that this could account for  
the differences in long-term trends in  $hmF2$  observed at different locations.

Subsequent analysis (Scott and Stamper, 2015) was conducted to investigate the long-term trends in annual/semiannual  
145 variability in  $f_oF2$  from 77 ionospheric monitoring stations around the world. By using Slough as a reference station, and  
correlating the long-term trends from other stations with it, strong regional variations were revealed in the data, which bore a  
striking similarity to the regional variation observed in long-term changes to the height of the ionospheric  $F2$  layer presented  
by Bremer et al. (2004). Scott and Stamper (2015) argued that since both the height and peak electron concentration of the  
150 ionospheric  $F2$  region are influenced by changes to thermospheric circulation and composition, the observed long-term and  
regional variability can be explained by such changes.

Rishbeth (1999) considered the results in  $hmF2$  long-term trends presented up to that date and discussed the challenges in  
extracting a reliable signal of the long-term ionospheric change induced by greenhouse warming. He argued that long-term  
sequences of ionosonde data are needed to address the question but that any data analysis must be "accurate and painstaking",  
155 with thought given to the subsequent analysis and interpretation of the data. Ulich et al. (2003) went further in considering  
some of the problems with identifying long-term trends in ionospheric data. They highlight the lack of consistency between  
results from different locations, the quality control of the data, the significance of any resulting trends, the reliance on empirical



formulae for calculating  $hmF2$  (including how they account for the presence of underlying ionisation) and the presence of other dominant signals in the data that lead to diurnal, seasonal and solar cycle variations.

160 The purpose of the current paper is to investigate the efficacy of deriving long-term ionospheric trends in  $hmF2$  using empirical formulae and to investigate the extent to which this can reconcile the difference in trends derived from the global network of ionospheric monitoring stations.

## 2 Estimating $hmF2$ from empirical formulae

While in more recent decades automatic scaling and inversion of ionograms have produced routine estimates of  $hmF2$ , for 165 historical data, this was not always the case. Even for those stations where the original analogue ionograms survive, retrospectively scaling and inverting these data would be prohibitively labour-intensive and time-consuming. Early on in ionospheric science, thought was given as to how to estimate  $hmF2$  values from existing scaled ionospheric parameters.

A first simple approach to the problem (Booker and Seaton, 1940; Appleton and Beynon, 1940) was to assume that the F2 layer electron concentration was parabolic with height (a so-called "parabolic model") and that collisions and the effects of the 170 Earth's magnetic field were ignored. From this, a relation between the true height,  $h$ , and the virtual height,  $h'$ , could then be derived.

Appleton and Beynon (1940) considered the relationship between the critical frequency for vertical incidence,  $f_oF2$ , and the maximum usable frequency,  $MUF$ , that can be reflected from the layer over a given distance. This relationship depends on the height of the layer, the thickness of the layer and, to a lesser extent, the presence of underlying ionisation. By international 175 agreement, for standard communications purposes, the  $MUF$  is considered over a distance of  $3000km$ . The ratio  $f_oF2/MUF$  is referred to as the  $M(3000)F2$  factor and is calculated according to a semi-empirical relation (e.g. Lockwood (1983)).

For a thin layer and a curved Earth, Appleton and Beynon (1940) derived the relationship;

$$hmF2 = 1500 / ((M3000F2^2 - 1)^{1/2}) - 176 \quad (1)$$

For a thick layer and curved Earth, Appleton and Beynon (1940) derived the following relation to estimate the true height of 180 the layer peak,  $hp$ ;

$$hp = 1153 / ((M^2 - 1)^{1/2}) - 100 \quad (2)$$

Shimazaki (1955) made simplifications to the theory, since Snell's law is invalid for a thick layer, Bouguer's rule (that the path of the ray is irrelevant) must be employed together with Martyn's equivalence theorem, applied to a curved Earth. The following relation was derived as a result;

$$185 \quad hmF2 = 1490 / M3000F2 - 176 \quad (3)$$





Dudeney (1974) showed that these assumptions should lead to an overestimate of  $hmF2$  of between 10 and 15 km. However, Shimazaki (1955) used data from a selection of stations representing a wide range of global locations and compared values obtained from his formula with those of Booker and Seaton (1940) and found no systematic offset. Dudeney (1974) suggested that this could be due to offsetting assumptions involving a simple parabolic layer, the lack of a magnetic field when deriving  $M(3000)F2$  (thus introducing a dependence on dip angle) and differences in the methods used of deriving  $M(3000)F2$  from actual ionograms. Dudeney (1974) concluded that the Shimazaki (1955) formulation is fundamentally inaccurate but that similar inaccuracies in the accepted method of determining  $M(3000)F2$  tend to compensate. Meanwhile, though the Appleton and Beynon (1940) formula was inherently more exact (with the  $1/(M^2 - 1)$  formulation being more accurate), it was of no practical use generally due to globally varying factors (such as the magnetic dip angle).

In their publication, Booker and Seaton (1940) recognised the need to correct for underlying ionisation in the  $E$  and  $F1$  layers. Vickers (1959) proposed a method that accounted for the  $F1$  layer ionisation but it was limited in that it could only be used when a scalable  $foF1$  parameter was visible on the ionogram (most often during the day in summer months) and the coefficients were strongly dependent on sunspot number, leading to further complex analysis.

Bradley and Dudeney (1973) found the simplest way to account for underlying ionisation was to use parabolic models for the  $E$  and  $F2$  layers and represent the interim ionisation with a linear increase in electron concentration. The height of the  $E$  layer peak was fixed at 120 km, with a thickness of 20 km. Trial and error showed that the best agreement occurred (with values of  $hmF2$  derived from ionogram inversion analysis) when the linear portion of the assumed underlying ionisation profile intersected the  $F2$  parabola where it equalled 2.89 times the peak E-layer electron concentration (equivalent to  $1.7foE$ ). They noted that the majority of  $foF1$  values on ionograms were scaled from minor fluctuations in electron concentration. They argued that it is the ionisation between the  $E$  and  $F2$  regions that contribute most to the group retardation of signals returned from the  $F2$  region, irrespective of the prominence of the  $F1$  ledge. In this way, they suggested  $F1$  ionisation could be accounted for by using the the more ubiquitous parameters  $foE$  and  $foF2$ .

Using synthetic ionograms that neglected the influence of the Earth's magnetic field, they found that their results were consistent with the following for  $x_E > 1.7$  (where  $x_E = foF2/foE$ )

$$hmF2 = a(M3000F2)^b \quad (4)$$

where  $a = 1890 - 355/(x_E - 1.4)$  and  $b = (2.5x_E - 3)^{-2.35} - 1.6$

They noted that  $x_E > 1.7$  is equivalent to about  $x_F \approx 1.2$  (where  $x_F = foF2/foF1$ ), well above the limit at which the shape of the underlying profile becomes important in practice.

Comparing the results from their formula with values obtained from ionogram inversion analysis for a number of different locations, seasons and points of the solar cycle, they found the agreement was generally very good, claiming that the presence of the  $F1$  layer had an insignificant effect on the group retardation.

While powerful, this method cannot be used when  $X_E < 1.7$ , which frequently occurs during the daytime summer. Neither does it account for the effects of the Earth's magnetic field.



Dudeny (1974) concluded that the best way to estimate  $hmF2$  is via ionogram inversion, though this is a slow and expensive  
220 process. The Bradley-Dudeny model (Bradley and Dudeny, 1973) is generally applicable over wide areas, though a model  
selected and calibrated to fit the ionosphere at a particular location is capable of higher accuracy (such as demonstrated by  
Vickers (1959)).

Dudeny (1974) considered a method that followed Shimazaki's original equation (Shimazaki, 1955) but applied a correction  
for the underlying ionisation using a value that assumes the contribution of  $f_oF1$  is negligible. To do this he differentiated  
225 Shimazaki's equation to obtain the relation;

$$\Delta h = (1490\Delta M)/M_o^2 \quad (5)$$

In this way, correcting for the underlying ionisation by considering the difference between modelled and observed heights  
as a function of  $\Delta M$ , means  $\Delta M$  can be considered a function of  $x_E$ . Whereas  $\Delta h$  is an inverse function of  $M$  and hence a  
direct function of  $hmF2$ . In this way, Dudeny (1974) established an empirical function of  $x_E$ , creating a single equation for  
230  $hmF2$  applicable to all epochs of the solar cycle. (but still not accounting for local variations in the Earth's magnetic field).

From his analysis, Dudeny (1974) derived two formulae;

$$hmF2 = 1490/(M3000F2 + \Delta M) - 176 \quad (6)$$

where  $\Delta M = (0.280 + / - 0.009)/(x_E - 1.200) - (0.028 + / - 0.010)$

or, more comprehensively;

$$235 \quad hmF2 = (1490.MF)/(M3000F2 + \Delta M) - 176 \quad (7)$$

where  $MF = M3000F2((0.0196M3000F2^2 + 1)/(1.2967M3000F2^2 - 1))^{1/2}$   $\Delta M = (0.253 \pm 0.008)/(x_E - 1.215)^{(0.012 \pm 0.009)}$

Dudeny (1974) state that the differences between these two equations are barely significant for most values of  $M(3000)F2$   
but become more important when  $M(3000)F2$  is small. Therefore for studies including solar cycle variations in  $hmF2$ , where  
240 extreme values of  $M(3000)F2$  are expected, the more complex relationships must be used.

For these relations, Dudeny (1974) estimates the uncertainty in  $hmF2$  to be  $\delta hmF2 \pm 89/M3000F2^2 km$ .

Dudeny (1974) concludes that calibration of this equation should be carried out for each individual station as it is probable  
that the  $\Delta M$  relation is a function of The Earth magnetic dip angle and and plasma gyro frequency. Through a comparison  
with the Bradley and Dudeny (1973) equation, Dudeny (1974) states that it should be possible to use the same coefficients  
245 with confidence over quite wide zones.

Subsequently, further refinements of the formula have been carried out, though a comprehensive review will not be given  
here. One popular formulation is that of Bilitza et al. (1979) which attempts to take account of geographic sensitivity to  
geomagnetic activity by using sunspot number as a proxy.





250 Bilitza et al. (1979) compare a wide variety of empirical  $hmF2$  formulae with incoherent scatter radar data (over periods of around 4 years from the 1960s and early 1970s) for Millstone Hill, Arecibo and Jicamarca. They conclude that the global ionosphere is best represented using either the Bradley and Dudeney (1973) model, or that of Bilitza and Eyfrig (1978).

McNamara (2008) used the international reference ionosphere (IRI) to generate ionospheric profiles against which the efficacy of the Dudeney (1974) and Bilitza et al. (1979) empirical  $hmF2$  formulae were tested. From these profiles they generated artificial ionograms for different times, seasons and points in the solar cycle. By scaling the necessary parameters from these 255 (including  $M(3000)F2$ ) they were able to use them to estimate  $hmF2$  using a variety of formulae. They concluded that the best agreement was found when considering the midnight  $F2$  layer using the simple approximation that  $hmF2$  was found at a virtual height where the plasma frequency was  $0.834 \times f_oF2$ , since at midnight, the layer approximates best to the assumption of a parabolic  $F2$  layer. However, this is not easily applied to the study of long-term change in the ionosphere since this parameter ( $hpF2$ ) was not routinely recorded and would require scaling from the original ionograms.

260 In the absence of  $hpF2$  values, McNamara (2008) concluded that the Dudeney (1974) model is better than the Bilitza et al. (1979) model for midnight ionograms. The scatter in the model errors is smallest at midnight, and is smaller for the Dudeney (1974) model (because the errors have a smaller solar-cycle variation). During the day, the Bilitza et al. (1979) formula gave the smaller range of errors because of the inclusion of a solar cycle term.

McNamara (2008) was also able to investigate the uncertainty in the values of  $M(3000)F2$ , which should be expected to 265 be at least as large as the standard scaling accuracy of  $\pm 0.05$ , with a superimposed random component. An uncertainty in  $M(3000)F2$  of  $\pm 0.1$  would lead to an uncertainty in  $hmF2$  of  $\pm 15km$ , though if these uncertainties were indeed random, this could be accounted for by considering monthly median values. McNamara (2008) cautions that the conclusions presented in their work are predicated on the assumption that the version of the IRI used was a better representation of the subpeak ionosphere than the empirical models of  $hmF2$ .

270 While analysis of long-term change in  $hmF2$  has been presented for many stations, no standard formula has been used to calculate  $hmF2$ . For the purposes of our analysis, which aims to investigate the presence of any long-term bias in empirical estimates of  $hmF2$  through comparison with heights determined by an extended sequence of data from Incoherent Scatter Radar, we will compare with the relation of Bradley and Dudeney (1973), presented in equation 4. Many authors have used this formulation, in particular Jarvis et al. (1998). It is useful for us to use this as a starting point for such comparisons with an ISR 275 since we wish to reproduce the analysis of Jarvis et al. (1998) here, in order to determine which elements can be interpreted as physical change within the ionosphere, and which are biases introduced by the assumptions used in formulating the empirical relationship between ionospheric parameters and  $hmF2$ . In keeping with Jarvis et al. (1998) we will estimate values of  $hmF2$  where  $f_oE$  is below the detection threshold of the ionosonde at night by assuming the low value of  $f_oE = 0.4MHz$ .

## 2.1 The Kokobunji ionosonde data

280 Routine observations of the ionosphere have been made using an ionosonde at Kokobunji, Japan (35.71 N, 139.49 E) since the International Geophysical Year in 1957. Scaled parameters from these hourly ionospheric soundings have been digitised and made available via the UK Solar System Data Centre ([www.ukssdc.ac.uk](http://www.ukssdc.ac.uk)). The peak electron concentrations of the  $E$  and



*F*2 layers (*f*<sub>o</sub>*E* and *f*<sub>o</sub>*F*2) along with the *M*(3000)*F*2 factor were used to calculate monthly median values for each hour. These were then used to estimate the true height of the *F*2 layer using the formula of Bradley and Dudeney (1973) as given in  
285 equation 4.

## 2.2 The Middle and Upper Atmosphere (MU) Radar

The Middle and Upper Atmospheric (MU) radar is located at Shigaraki MU observatory, Shigaraki, Japan. Being located at latitude 34.85° N and longitude of 136.12° E, this is at a similar latitude to Kokobunji and about 310km to the west. For 2004 (the centre of the interval over which data from the two stations are compared) the International Geomagnetic Reference Field  
290 (IGRF) gives the geomagnetic coordinates of the Kokobunji ionosonde to be 26.78° N and 208.22° E and of the MU radar to be 25.65° N and 205.24° E. Designed for both middle and upper atmospheric studies, it has been routinely making observations of the ionosphere using incoherent scatter since 1986. True incoherent scatter occurs when an electromagnetic wave excites electrons within a plasma. Each electron acts as an antenna that re-radiates the wave, with the thermal and bulk motion of the plasma Doppler shifting the original signal. The received signal is a superposition of the re-radiated waves from all the  
295 electrons in the line-of-sight of the incoming wave in the range "gate" set by the pulse delay range that the received signals are integrated over. In the ionosphere, While the heavier positive ions within the plasma are not excited directly by the radio wave, they influence the motion of the electrons, thereby modifying the received signal spectrum. If the transmitted frequency corresponds to wavelengths significantly greater than the Debye length of the plasma, the scatter is not truly incoherent, but rather occurs preferentially from ion-acoustic waves within the plasma, resulting in a characteristic 'double-humped' spectrum  
300 corresponding to the upwards and downwards propagating ion-acoustic waves of the appropriate wavelength. In this way, incoherent scatter enables routine measurement of electron concentration, the bulk motion of the plasma and the ion and electron temperatures.

The MU radar transmits in the VHF radio spectrum at a frequency of 46.5MHz (3.5MHz bandwidth and 1MW peak output power). The antenna field consists of 475 antennas arranged in a circular array with a diameter of 103metres. Fast beam  
305 steering enables various observation configurations. Ionospheric observations are routinely made with the radar in Incoherent Scatter Radar (ISR) mode. These consist of a sequence of four beam directions, with the azimuth and zenith angles of the beams of (355.0, 20.0), (85.0, 20.0), (175.0, 20.0), and (265.0, 20.0), degrees respectively. When operating in ISR mode, the radar can make measurements of electron and ion temperatures, plasma velocity and echo power density. The echo power data show the intensity of electromagnetic waves reflected from the ionosphere between 80 and 1,200km. The heights recorded  
310 by the ISR are not subject to the same delays as with the ionosonde data since the transmitted frequencies are far greater than ionospheric plasma frequencies. However, at 46.5MHz there will still be small delays that will result in the systematic increase in measurements of F2 layer height of the same order as the height resolution of the radar ( $\approx 4.5km$ ). For clarity, such delays are not considered in the main analysis of the current paper, since their inclusion does not significantly affect the results. Modified results that include an estimate of the expected delay are discussed in the conclusions.

315 The ISR mode is run on a campaign basis, with a typical run lasting from several hours to over a day. The data are made available as hourly averages of height versus received power (in decibels) for the four antenna positions. For the purposes of



our analysis, data from the four beams were first converted from decibels to a received power of arbitrary units following the method detailed by Sato et al. (1989). These height profiles were then averaged to reduce any random errors. The system noise for each combined height profile was then estimated from the average power returned from heights above  $700\text{km}$  (which are considered to contain no signal). This noise was then subtracted from the received powers which were then range corrected. The resulting power profiles can be converted to absolute electron concentration through calibration with a measure of absolute electron concentration (such as from an ionosonde) but this was not necessary for the present analysis since it was only the height of the ionospheric  $F2$  layer that was of interest, not the electron concentration. The  $F2$  peak in each profile was then identified as the largest range-corrected power in each profile occurring between altitudes of  $180$  and  $500\text{km}$ . This window was selected to be as wide as possible without potential contamination from strong sporadic E layers. In order to suppress estimates from noisy profiles, data points with a signal-to-noise-ratio (SNR) below  $5\%$  were excluded from the analysis.

For comparison with the  $hmF2$  values estimated from the ionosonde data, monthly means were calculated for each hour of ISR data. The radar is not run in ISR mode as routinely as the ionosonde generates ionograms, but over the 35 years of data used in this study, observations have been made in  $48\%$  of the 10080 bins (monthly averages for each hour over 35 years). While monthly median values are calculated for the ionosonde parameters, this is to protect against outliers in ionospheric concentrations caused by short-lived space weather events that are not representative of the monthly data. For the ISR data, measuring  $hmF2$  directly, the number of data points per bin is small and so the median is inappropriate. That having been said, the mean and median values were significantly different in only 17 out of the 4853 bins containing data. When the ISR data are averaged annually, there is no significant difference between the arithmetic mean and median values.

## 3 Results

### 3.1 Seasonal and diurnal comparison

Hourly monthly median  $hmF2$  values derived from the Kokubunji ionosonde data using the model of Bradley and Dudeney (1973) are presented in figure 1 (top panel). These are compared with hourly mean  $hmF2$  values derived from the MU radar (lower panel). Both data sequences show a clear solar cycle trend, as well as a decreasing trend visible in both sequences from the start of routine MU radar observations in 1986.

The  $hmF2$  values from the two datasets are compared in figure 2 for the 35 years when the two datasets overlap (1986-2020). Daytime data (for which the solar zenith angle,  $sza > 100^\circ$ ) are shown as black points, twilight data ( $90^\circ \leq sza \leq 100^\circ$ ) are shown in yellow while nighttime data ( $sza > 100^\circ$ ) are shown as cyan points. As expected, there is a strong similarity between the two datasets, although there is much more scatter in the twilight and night-time estimates of  $hmF2$ . It is likely that this scatter results from the assumption that  $f_oE = 0.4\text{MHz}$  which not only affects the night-time estimates, but also those where  $f_oE$  is below the measurement threshold of the ionosonde itself. Conducting a robust linear fit to all the data (to minimise the influence of outliers) results in a best-fit line with a gradient of  $0.71 \pm 0.01$  and an offset of  $86.15 \pm 1.82\text{km}$ . Restricting the fit to consider just the daytime points, the relationship improves considerably, with a gradient of  $0.86 \pm 0.1$  and offset of  $37.63 \pm 2.01$ .



350 In order to investigate whether this difference was due to seasonal or diurnal biases between the two data sets, monthly averages were calculated for each hour, averaging over the 35 years for which there was common data. The results are presented in figure 3. While the broad distributions are largely similar in both data sets (higher  $hmF2$  at night), there are differences. The ISR shows more distinct peaks in  $hmF2$  at the equinoxes (months 3 and 9) while the ionosonde-derived  $hmF2$  values show a stronger peak around mid-day in the summer months. We next investigated whether the assumptions made about  
355 the underlying ionisation in the empirical calculation of  $hmF2$  could be the source of this bias. To do this, we plotted the difference between these two data sets against the ratio of  $f_oF2/f_oF1$  values. The results are presented in figure 4. While there is no significant difference between the two distributions for values of the  $f_oF2/f_oF1$  ratio above 1.6, below this, the presence of an  $f_oF1$  layer significantly affects the ionosonde-derived  $hmF2$  values due to the presence of underlying ionisation that is unaccounted for in the empirical formula. A line was fitted to the values with a ratio below 1.6 (gradient  
360  $231 \pm 21$ , offset  $-356 \pm 31km$ ) and this relationship was used to correct for the presence of  $f_oF1$  in the ionosonde-derived estimates of  $hmF2$ . The revised seasonal and diurnal distribution is presented in figure 5. Comparing with the distribution of ISR-derived  $hmF2$  values presented in the lower panel of figure 3, it can be seen that corrected ionosonde-derived  $hmF2$  daytime summer values (where  $f_oF1$  is most likely to be observed) are now in much closer agreement with the ISR values. While the presence of  $f_oF1$  values during the day are an indication of changes in thermospheric composition, this has not  
365 corrected for the difference in nighttime  $hmF2$  values since  $f_oF1$  is only visible during daylight hours. Nevertheless, changes to the thermospheric composition will still be present at night, affecting the loss-rate of ionisation which could potentially introduce a bias into the derivation of  $hmF2$  values through changes to the distribution of underlying ionisation. Additionally, it has been shown that there is a greater uncertainty in the empirical equation via the approximation of a fixed  $f_oE$  value of  $0.4MHz$  at night.

### 370 3.2 Long-term bias

Having established that the presence of an  $F1$  layer can introduce systematic errors in to the empirical formula on a seasonal and diurnal basis, it is pertinent to the discussion of long-term change in the ionosphere to now consider how such a bias may influence the long-term trends in  $hmF2$  values derived via an empirical formula. Figure 6 presents the  $f_oF2/f_oF1$  ratio against year for hourly monthly median values (top panel), annual average (middle panel) and the percentage of observations  
375 where  $f_oF1$  is present, for which the ratio is  $\leq 1.6$  (as identified in Figure 4). It can be seen that there is a strong solar cycle dependence in this ratio, together with longer-term changes, particularly the apparent step change since the year 2000. The result of this is that some years will be far more susceptible to the systematic errors introduced into the empirical formula by the presence of  $f_oF1$ . The lower panel demonstrates that the percentage of  $f_oF2/f_oF1$  values (for which  $f_oF1$  is present) falling below the threshold of 1.6 can vary from around 10 to 100%.

380 The relationship between the  $hmF2$  systematic error and the  $f_oF2/f_oF1$  ratio established above was used to correct affected daytime values within the hourly monthly median  $hmF2$  values. When plotted against the ISR  $hmF2$  values (figure 7, the correction results in a revised gradient of  $0.89 \pm 0.01$  with an offset of  $30.32 \pm 2.28km$ . While this has improved the relationship between the empirically derived and directly measured  $hmF2$  values, the remaining offset is not 1:1. This is



385 unsurprising since there are other approximations that have been made when determining the coefficients within the empirical relation (which are likely specific to the dip angle of the local magnetic field) and in deriving  $M(3000)F2$  values from the ionograms (which does not account for the presence of the magnetic field). In addition, we have not corrected for the small but systematic bias in  $hmF2$  introduced by the signal delay in the ISR data.

It can be seen from figure 5 that the night-time ionosonde-derived  $hmF2$  values are generally still lower than those measured by the ISR. As shown in figure 2, using a value of  $f_oE = 0.4MHz$  in the empirical formula tends to introduce more uncertainty into the  $hmF2$  estimates which results in an underestimate of the F2 layer height on average.

### 3.3 Influence of the Earth's magnetic field on long-term $hmF2$ estimates

Standard calculations of  $M(3000)F2$  do not take account of the influence of the Earth's magnetic field on radio propagation and it has long been known that this can introduce a bias into the estimation of this parameter from ionograms (Davies, 1959). More recently, Elias et al. (2017) have modelled this bias and quantified the subsequent error introduced into estimates of  $hmF2$ . In order to estimate the influence of the magnetic field on  $hmF2$  calculations for the location used in this study, the international geomagnetic reference field (IGRF, Thébault et al. (2015)) was used to determine long-term magnetic field variations at an altitude of 250km above Kokubunji. Throughout the epoch of this study, the inclination has remained relatively stable, declining from 48.7° to 48.4° between 1957 and 1980, subsequently rising to 49.6° by 2020. Using the figure presented in Elias et al. (2017), this would result in a systematic offset in  $hmF2$  of  $\leq 1km$ , well within the uncertainties of the measurements. Further to this, modelling work by Cnossen and Richmond (2008) and Elias (2009) indicates that changes to the Earth's magnetic field over Kokubunji would not be expected to affect the observed values of  $hmF2$  through thermospheric dynamics for the epoch covered by this study. It is therefore assumed that there is no measurable bias caused by magnetic field changes in the long-term variation in  $hmF2$ .

### 3.4 The impact of $f_oF1$ on the long-term drift in estimates of $hmF2$

405 Having established that the presence of an F1 layer, itself an indication of a change in thermospheric composition, can lead to a systematic bias when using an empirical formula to estimate  $hmF2$ , this raises the question as to whether such a bias would be introduced into the study of long-term change in the height of the F2 layer.

In order to investigate this, the relationship between the ISR and ionosonde-derived  $hmF2$  values was determined for each of the 35 years of common data. For each year, monthly median ionosonde-derived  $hmF2$  values were plotted against mean ISR measurements for all hours and months where there were data from both instruments. For each year, a linear fit was made between ionosonde-derived and ISR  $hmF2$  values. The resulting gradient and offset of each fit were used to reconstruct the percentage error in  $hmF2$  values for an arbitrary height of 250km. The results of this analysis are presented in Figure 8 (a). It can be seen that there are solar cycle variations in the model error with an amplitude of  $\pm 10\%$  ( $\pm 25km$  at 250). Moreover, there is a long-term drift in this error which would undoubtedly introduce a bias into any estimates of long-term change in the height of the F2 layer. The question then arises as to what could be the cause of this long-term change in the formula error. Figure 8 (c) presents the annual average of the geophysical  $am$  index (Lockwood et al., 2019). There is a strong and significant



correlation ( $0.77, p \ll 0.0001$ ), between the two, suggesting that it is geomagnetic activity that is driving this variation in the accuracy of the empirical formula. If this long-term bias is consistent with the seasonal and diurnal bias of  $hmF2$  estimates demonstrated in the earlier section of this paper, it would be reasonable to assume that the formula is being affected by changes to the underlying ionisation profile, introduced by long-term changes in thermospheric composition. Figure 8 (b) presents a qualitative proxy for the annual average thermospheric composition calculated from monthly median noon  $f_oF2$  values scaled by the solar  $f_{10.7cm}$  flux (Wright and Conkright, 2001). It can be seen that this proxy reveals very similar characteristics of a solar-cycle variation combined with a long-term decline (correlation  $0.835, p \ll 0.0001$ ). More directly related to the earlier result that a bias is introduced into the empirical  $hmF2$  formula by the presence of an  $F1$  layer, figure 8 (d) presents the annual average ratio of  $f_oF2/f_oF1$ . This too demonstrates similar solar cycle variations combined with a long-term decrease (correlation  $0.862, p \ll 0.0001$ ).

The sensitivity of thermospheric composition changes to geomagnetic activity varies with geomagnetic latitude (e.g. Zuzic et al. (1997)), with a station at low geomagnetic latitude being less prone to changes in molecular species at F-region altitudes than a station at a high geomagnetic latitude.

For example, Slough/Chilton, is a mid-latitude station in a longitude sector near to the geomagnetic pole ( $\approx 48 - 50$  N). Here there is an annual variation in ionisation, with ionospheric densities being greatest in the winter. In the summer, the greater concentration of molecular species in the thermosphere increases the ionospheric loss rate, resulting in lower F-region ionospheric densities in the summer months where the proportion of molecular species is relatively high. In the winter months, down-welling of the meridional thermospheric circulation results in a thermospheric composition dominated by atomic species which have a lower loss rate. This seasonal change in composition exceeds the variation in ion production due to the seasonal change in solar zenith angle over the same period.

When a station is far enough from the magnetic pole that compositional changes between equinox and winter months are relatively small compared with the associated change in solar zenith angle, a semiannual variation in  $f_oF2$  results, such as is seen at Stanley in the Falkland Islands ( $\approx 35 - 39S$ ).

Such differences are also likely to influence the relative values of the  $f_oF2/f_oF1$  ratio at these stations, since  $f_oF2$  will be suppressed at Slough/Chilton during the summer months when  $f_oF1$  is at its peak. Figure 9 presents the mean annual  $f_oF2/f_oF1$  ratio calculated for Slough/Chilton (top panel) and Stanley (lower panel). If 1.6 is taken as the critical value below which a bias is introduced into the empirical formula used to calculate  $hmF2$  (shown in the figure as a dash-dot line) it can be seen that Slough/Chilton will be far more susceptible to these biases than Stanley, where the mean  $f_oF2/f_oF1$  ratio is higher and a greater proportion of the values lie above this threshold. In addition, both stations exhibit some long-term change in this ratio which would introduce further bias into any estimates of long-term trends in  $hmF2$ . Such regional differences will need to be accounted for in any global analysis of  $hmF2$  trends.





### 3.5 Accounting for signal delay in the estimate of $hmF2$ in the MU radar ISR data

As discussed previously, the above analysis has assumed that the propagation of the ISR radar pulses was not delayed by the presence of underlying ionisation. Which, for the frequency of the MU radar (46.5 MHz) is expected to introduce a small but systematic offset.

In order to estimate this offset, the simplified Appleton-Hartree equation was applied, where;

$$\mu^2 = 1 - kN/f^2 \quad (8)$$

where  $k = 80.5$ ,  $N$  is the electron concentration per  $m^3$  and  $f$  is the radar frequency. Applying the binomial expansion, this can be approximated to;

$$\mu = 1 - 40.3N/f^2 \quad (9)$$

Here, the second term on the right-hand side of the equation represents the range bias introduced as the radio wave passes through a plasma. In this way, 1  $TEC$  unit ( $1e16$  electrons per  $m^2$ ) delays the ISR signal by approximately  $(1e16 * 40.3)/(46.5e6)^2 = 186m$ .

In order to estimate the likely impact of such a bias in the data being considered, the 2016 International Reference Ionosphere (IRI2016) was used to generate electron concentration profiles at the location of the MU radar for dates between 1986 and 2020, corresponding to each month and hour considered in the study. Each ionospheric profile was then integrated from an altitude of 80 km up to the height of the maximum electron concentration in order to estimate the integrated range bias (doubled to account for the two way travel of the radio pulse).

The resulting values vary between 0.6 and 11.5 km with a median value of 1.47 km varying as a function of peak electron concentration which, as expected, varies with time of day, season and solar cycle.

The matrix of height offsets was then subtracted from the  $hmF2$  hourly monthly means derived from the ISR data and the analysis was repeated. While the underlying conclusions concerning the impact of  $f_oF1$  on the empirical  $hmF2$  formula are unaffected, the systematic reduction in radar-derived values of  $hmF2$  resulted in an improved relationship between the ionosonde and ISR derived heights. Before correcting for the presence of  $f_oF1$ , the revised gradient for daytime  $hmF2$  increases by 0.3 to  $0.89 \pm 0.01$ , while the equivalent after correcting for the presence of  $f_oF1$  increases by 0.3 to  $0.92 \pm 0.01$ .

## 4 Conclusions

Empirical formulae used to estimate the height of the ionospheric F2 layer from standard parameters, scaled from ionograms, have necessarily had to make some assumptions about the underlying ionisation profile. We have shown that, for at least one of the established empirical formulae, that diurnal, seasonal and long-term biases are introduced into estimates of  $hmF2$  that are of similar, if not greater, magnitude than those expected to be introduced by the long-term cooling resulting from





increased levels of  $CO_2$  and  $CH_4$  in the lower atmosphere. While in the case of the Kokubunji station, the long-term bias is well correlated with long-term changes in geomagnetic activity, the physical mechanism is via changes to the underlying ionisation, driven by variation in thermospheric composition. This leads to diurnal, seasonal, and long-term variation in the  $f_oF_2/f_oF_1$  ratio that is not accounted for in the empirical formula. While the wider family of empirical formulae have not been tested in this work, there is evidence (McNamara, 2008) that at least some of these empirical formulae exhibit seasonal bias. Furthermore, there is evidence that, while being driven by geomagnetic activity, long-term change in ionospheric composition can be geographically localised, with individual stations exhibiting a wide range of responses to geomagnetic activity (Scott et al., 2014; Scott and Stamper, 2015). We conclude that the lack of consistency in global estimates of long-term changes in  $hmF_2$  results from the localised nature of the long-term changes in thermospheric composition not accounted for in the empirical formula used.

Jarvis et al. (1998) reported an altitude-dependence in their estimates of long-term change in  $hmF_2$  and hypothesised physical mechanisms that would explain this. Our results indicate that the bias introduced into the formula affects the percentage uncertainty in the estimate of  $hmF_2$ , which would lead to a bias that would also be altitude dependant.

It may be possible to use the relationship between the  $f_oF_2/f_oF_1$  ratio and the formula bias to correct for long-term changes in thermospheric composition for this station, and it is also likely that the  $f_oF_2/f_oF_1$  ratios at other stations could be used to account for the global variations in this bias to produce a unified estimate of the rate of long-term change in  $hmF_2$ . Caution should be used in such an exercise however, since the bias in the formula varies with season and time of day. In addition, the formula used was calibrated for a specific station and the sensitivity to these biases may vary with location. Other variations on the formula should be tested in this way to determine their relative sensitivities to compositional effects. It would be interesting to see if the biases determined in the present study vary with latitude by conducting similar calibrations using other ISR stations.

With the potential for biases within these empirical  $hmF_2$  formulae, the ideal approach would be to determine such trends from alternative sources such as directly from ISR measurements (which, as pointed out by Rishbeth (1999) will require a few more decades of measurements before any trends can be considered significant) or through the labour-intensive process of inverting ionogram profiles. While this latter suggestion is theoretically possible for stations such as Slough/Chilton for which the original ionograms still exist, such a task is currently beyond the scope of this analysis, requiring careful digitisation, scaling and verification across many generations of instruments and data formats.

While this work has not addressed any potential bias introduced by long-term changes to thermospheric circulation or geomagnetic field, it has nonetheless demonstrated a bias in the formula that, through long-term changes in thermospheric composition, can lead to localised biases in the estimates of  $hmF_2$  which in turn can explain the lack of global consensus in long-term changes in the height of the ionosphere. Importantly, the results from this paper show that diurnal, seasonal and long-term biases are introduced into estimates of trends in ionospheric heights that are of similar, if not greater, magnitude than those expected to be introduced by the long-term thermospheric cooling. These analysis issues must be addressed before ionospheric observations can be correctly interpreted in relation to long-term climate models.



*Code and data availability.* Software used in the analysis of these data is available via <https://github.com/cscott42/hmF2CalibrationCode> (This will be deposited on Zenodo on acceptance of the paper). MU radar data was provided by the Research Institute for Sustainable Humanosphere of Kyoto University can be obtained from their website at <https://www.rish.kyoto-u.ac.jp/mu/isdata/>. Ionospheric data used in this analysis are available via the UK Solar System Data Centre at <https://www.ukssdc.ac.uk>.

515 *Author contributions.* C. J. Scott lead on the data analysis and interpretation. M. N. Wild advised on and provided the ionosonde data, L. A. Barnard and B. Yu contributed to the data analysis, T. Yokoyama advised on the analysis of MU radar data, M. Lockwood advised on analysis and geomagnetic indices, C. Mitchel conducted analysis on the range correction of MU radar data, J. Coxon provided early insight into data analysis methods and A. Kavanagh provided access to important reference material.

*Competing interests.* At least one of the (co-)authors is a member of the editorial board of *Annales Geophysicae*.

520 *Acknowledgements.* The authors would like to thank the Research Institute for Sustainable Humanosphere of Kyoto University for providing the MU radar data, WDC for Ionosphere and Space Weather, Tokyo, National Institute of Information and Communications Technology for providing the Kokubunji ionosonde data, which was also made available through the UK Solar System Data Centre. This work was funded under the UKRI grant NE/W003384/1.



## References

- 525 Appleton, Edward. V. and Beynon, W. J. G.: The Application of Ionospheric Data to Radio-Communications Problems: Part I, *Proc. Physcs Soc*, 52, 518–33, 1940.
- Bilitza, D. and Eyfrig, R.: Modell Zur Darstellung Der Hone Des F2-maximums Mit Hilfe Des M(3000)F2-Wertes Der CCIR, *Kleinheubacher Berichte*, 21, 167–174, 1978.
- Bilitza, D., Sheikh, N. M., and Eyfrig, R.: A Global Model for the Height of the F2-peak Using M3000 Values from the CCIR Numerical  
530 Map, *Telecommunication Journal*, 46, 549–553, 1979.
- Booker, H. G. and Seaton, S. L.: The Relation between Actual and Virtual Ionospheric Height, *Phys. Rev*, 57, 58–76, 1940.
- Bradley, P. A. and Dudeney, R., J.: A Simple Model Representation of the Electron Concentration of the Ionosphere, *Journal of Atmospheric and Terrestrial Physics*, 35, 2131–2146, 1973.
- Bremer, J.: Ionospheric Trends in Mid-Latitudes as a Possible Indicator of the Atmospheric Greenhouse Effect, *J. Atmos. Terr. Phys.*, 54,  
535 1505–1511, 1992.
- Bremer, J.: Trends in the Ionospheric E- and F-regions over Europe, *Ann. Geophysicae*, 16, 986–996, 1998.
- Bremer, J., Alfonsi, L., Bencze, P., Lastovicka, J., Mikhailov, A. V., and Rogers, N.: Long-Term Trends in the Ionosphere and Upper Atmosphere Parameters, *Annals of Geophysics*, 47, 1009–1029, 2004.
- Cnossen, I. and Richmond, A. D.: Modelling the Effects of Changes in the Earth’s Magnetic Field from 1957 to 1997 on the Ionospheric  
540 hmF2 and foF2 Parameters, *Journal of Atmospheric and Solar-Terrestrial Physics*, 70, 1512–1524, 2008.
- Davies, K.: The Effect of the Earth’s Magnetic Field on m.u.f. Calculations, *Journal of Atmospheric and Solar-Terrestrial Physics*, 16, 187–189, 1959.
- Dudeney, R., J.: A Semi-Empirical Method for Estimating the Height and Semi-Thickness of the F2-layer at the Argentine Islands, *Graham Land, British Antarctic Survey Scientific Reports*, 1974.
- 545 Dungey, J. W.: Interplanetary Magnetic Field and the Auroral Zones, *Physical Review Letters*, 6, 47–48, <https://doi.org/10.1103/physrevlett.6.47>. ISSN 0031-9007, 1961.
- Elias, A. G.: Trends in the F2 Ionospheric Layer Due to Long-Term Variations in the Earth’s Magnetic Field, *Journal of Atmospheric and Solar-Terrestrial Physics*, 71, 1602–1609, 2009.
- Elias, A. G., Zossi, B. S., Yigit, Y., Saavedra, Z., and de Haro Barbas, B. F.: Earth’s Magnetic Field Effect on MUF Calculation and  
550 Consequences for hmF2 Trend Estimates, *Journal of Atmospheric and Solar-Terrestrial Physics*, 163, 114–119, 2017.
- Jarvis, M., Jenkins, B., and Rodger, A.: Southern Hemisphere Observations of a Long-Term Decrease in F Region Altitude and Thermospheric Wind Providing Possible Evidence for Global Thermospheric Cooling, *JGR*, 130, 20 774–20 787, 1998.
- King, G. A. M.: The Ionospheric F-region during a Storm, *Planetary and Space Science*, 9, 95–98, [https://doi.org/10.1016/0032-0633\(62\)90179-4](https://doi.org/10.1016/0032-0633(62)90179-4), 1963.
- 555 Lastovicka, J.: Trends in the Upper Atmosphere and Ionosphere: Recent Progress, *Journal of Geophysical Research: Space Physics*, 118, 3924–3935, <https://doi.org/10.1002/jgra.50341>, 2013.
- Lockwood, M.: A Simple M-factor Algorithm for Improved Estimation of the Basic Maximum Usable Frequency of Radio Waves Reflected from the Ionospheric F Region, *Proc. IEE - F*, 130, 296–302, <https://doi.org/10.1049/ip-f-1.1983.0049>, 1983.
- Lockwood, M., Chambodut, A., Finch, I. D., Barnard, L. A., Owens, M. J., and Haines, C.: Time-of-day / Time-of-year Response Functions  
560 of Planetary Geomagnetic Indices, *J. Space Weather Space Clim.*, 9, <https://doi.org/10.1051/swsc/2019017>, 2019.



- McCrea, I. W., Lester, M., Robinson, T. B., Wade, N. M., and Jones, T. B.: On the Identification and Occurrence of Ion Frictional Heating Events in the High-Latitude Ionosphere, *Journal of Atmospheric and Terrestrial Physics*, 53, 587–597, [https://doi.org/10.1016/0021-9169\(91\)90087-N](https://doi.org/10.1016/0021-9169(91)90087-N), 1991.
- McNamara, L. F.: Accuracy of Models of hmF2 Used for Long-Term Trend Analyses, *Radio Science*, 43,   
565 <https://doi.org/doi:10.1029/2007RS003740>, 2008.
- Mikhailov, A. V.: Ionospheric Long-Term Trends: Can the Geomagnetic Control and the Greenhouse Hypotheses Be Reconciled?, *Annales Geophysicae*, 24, 2533–2541, 2006.
- Mikhailov, A. V. and Marin, D.: An Interpretation of the foF2 and hmF2 Long-Term Trends in the Framework of the Geomagnetic Control Concept, *Annales Geophysicae*, 19, 733–748, <https://doi.org/10.5194/angeo-19-733-2001>, 2001.
- 570 Pulkkinen, T.: Space Weather: Terrestrial Perspective, *Living Rev. Sol. Phys.*, 4, <https://doi.org/10.12942/lrsp-2007-1>, 2007.
- Rishbeth, H.: Basic Physics of the Ionosphere: A Tutorial Review, *Journal of the Institute of Electronic and Radio Engineers*, 58, 1988.
- Rishbeth, H.: A Greenhouse Effect in the Ionosphere?, *Planetary and Space Science*, 38, 945–948, 1990.
- Rishbeth, H.: Chances and Changes: The Detection of Long-term Trends in the Ionosphere, *EOS*, 80, 1999.
- Rishbeth, H. and Garriott, O.: Introduction to Ionospheric Physics, *International Geophysics*, 1969.
- 575 Rishbeth, H., Gordon, R., Rees, D., and Fuller-Rowell, T. J.: Modelling of Thermospheric Composition Changes Caused by a Severe Magnetic Storm, *Planetary and Space Science*, 33, 1283–1301, [https://doi.org/10.1016/0032-0633\(85\)90007-8](https://doi.org/10.1016/0032-0633(85)90007-8), 1985.
- Roble, R. G. and Dickinson, R. E.: How Will Changes in Carbon Dioxide and Methane Modify the Mean Structure of the Mesosphere and Thermosphere, *Geophys. Res. Lett.*, 16, 1441–1444, 1989.
- Santer, B. D., Po-Chedley, S., Zhao, L., Zou, C.-Z., Fu, Q., Solomon, S., Thompson, D. W. J., Mears, C., and Taylor,   
580 K. E.: Exceptional Stratospheric Contribution to Human Fingerprints on Atmospheric Temperature, *P.N.A.S.*, 120, e2300758 120, <https://doi.org/10.1073/pnas.2300758120>, 2023.
- Sato, T., Ito, A., Oliver, W. L., Fukao, S., Tsuda, T., Kato, S., and Kimura, I.: Ionospheric Incoherent Scatter Measurements with the Middle and Upper Atmosphere Radar: Techniques and Capability, *Radio Science*, 24, 85–98, 1989.
- Schwenn, R.: Space Weather: The Solar Perspective, *Living Rev. Sol. Phys.*, 3, <https://doi.org/10.12942/lrsp-2006-2>, 2006.
- 585 Scott, C. and Stamper, R.: Global Variation in the Long-Term Seasonal Changes Observed in Ionospheric F Region Data, *Annales Geophysicae*, 33, 449–455, <https://doi.org/10.5194/angeo-33-449-2015>, 2015.
- Scott, C., Stamper, R., and Rishbeth, H.: Long-Term Changes in Thermospheric Composition Inferred from a Spectral Analysis of Ionospheric F-region Data, *Annales Geophysicae*, 32, 113–119, <https://doi.org/10.5194/angeo-32-113-2014>, 2014.
- Shangguan, M., Wuke, W., and Shuanggen, J.: Variability of Temperature and Ozone in the Upper Troposphere and Lower Stratosphere from   
590 Multi-Satellite Observations and Reanalysis Data, *Atmospheric Chemistry and Physics*, 19, 6659–6679, <https://doi.org/10.5194/acp-19-6659-2019>, 2019.
- Shimazaki, T.: Worldwide Variations in the Height of the Maximum Electron Density in the Ionospheric F2 Layer, *Journal of Radio Research Labs Japan*, 2, 85–97, 1955.
- Thébaud, E., Finlay, C. C., Beggan, C. D., Alken, P., Aubert, J., Barrois, O., Bertrand, F., Bondar, T., Boness, A., Brocco, L., Canet, E.,   
595 Chambodut, A., Chulliat, A., Coisson, P., Civet, F., Du, A., Fournier, A., Fratter, I., Gillet, N., Hamilton, B., Hamoudi, M., Hulot, G., Jager, T., Korte, M., Kuang, W., Lalanne, X., Langlais, B., Léger, J.-M., Lesur, V., Lowes, F. J., Macmillan, S., Mandea, M., Manoj, C., Maus, S., Olsen, N., Petrov, V., Ridley, V., Rother, M., Sabaka, T. J., Saturnino, D., Schachtschneider, R., Sirol, O., Tangborn, A.,



- Thomson, A., Tøffner-Clausen, L., Vigneron, P., Wardinski, I., and Zvereva, T.: International Geomagnetic Reference Field: The 12th Generation, *Earth Planets Space*, 67, 79, <https://doi.org/10.1186/s40623-015-0228-9>, 2015.
- 600 Ulich, T., Clilverd, M. A., and Rishbeth, H.: Determining Long-Term Change in the Ionosphere, *EOS*, 84, 581–585, 2003.
- Vickers, M. D.: The Effect of the F1 Layer on the Calculation of the Height of the F2-layer, *J. Atmos. Terr. Phys.*, 16, 103–105, 1959.
- Wright, J. W. and Conkright, R. O.: Prospects for an Ionospheric Index of Neutral Thermospheric Composition, with Space-Weather Applications, *Journal of Geophysical Research: Space Physics*, 106, 21 063–21 075, <https://doi.org/10.1029/2000JA000215>, 2001.
- Xu, Z.-W., Wu, J., Igarashi, K., Kato, H., and Wu, Z.-S.: Long-Term Ionospheric Trends Based on Ground-Based Ionosonde Observations at  
605 Kokubunji, Japan, *Journal of Geophysical Research*, 109, <https://doi.org/10.1029/2004JA010572>, 2004.
- Zuzic, M., Scherliess, L., and Prolss, G. W.: Latitudinal Structure of Thermospheric Composition Perturbations, *Journal of Atmospheric and Solar-Terrestrial Physics*, 59, 711–724, [https://doi.org/10.1016/S1364-6826\(96\)00098-3](https://doi.org/10.1016/S1364-6826(96)00098-3), 1997.

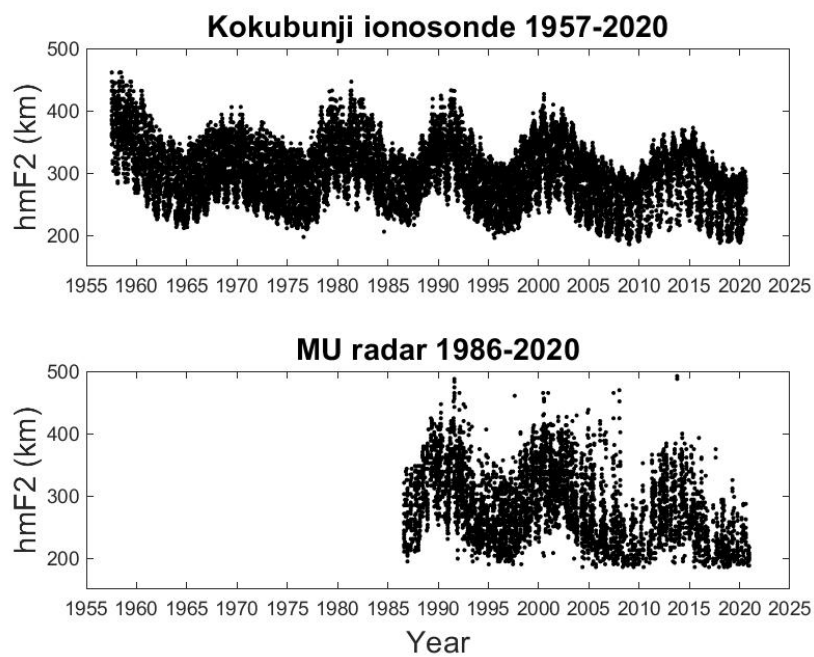


**Figure 1.** Hourly monthly median  $hmF2$  values derived from the Kokubunji ionosonde data (top panel). compared with hourly mean  $hmF2$  values derived from the MU radar (lower panel).

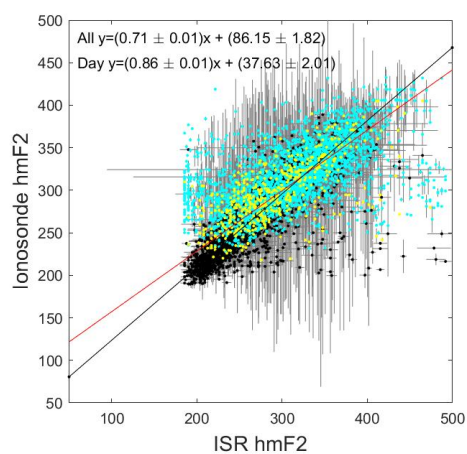


**Figure 2.** Hourly monthly median  $hmF2$  values derived from the Kokubunji ionosonde data versus hourly mean  $hmF2$  values derived from the MU radar. A linear fit between the data sets for all data (red line) has a gradient of  $0.71 \pm 0.01$  while for daytime only (solar zenith angle  $> 100^\circ$ , black line) the gradient is  $0.86 \pm 0.01$ .



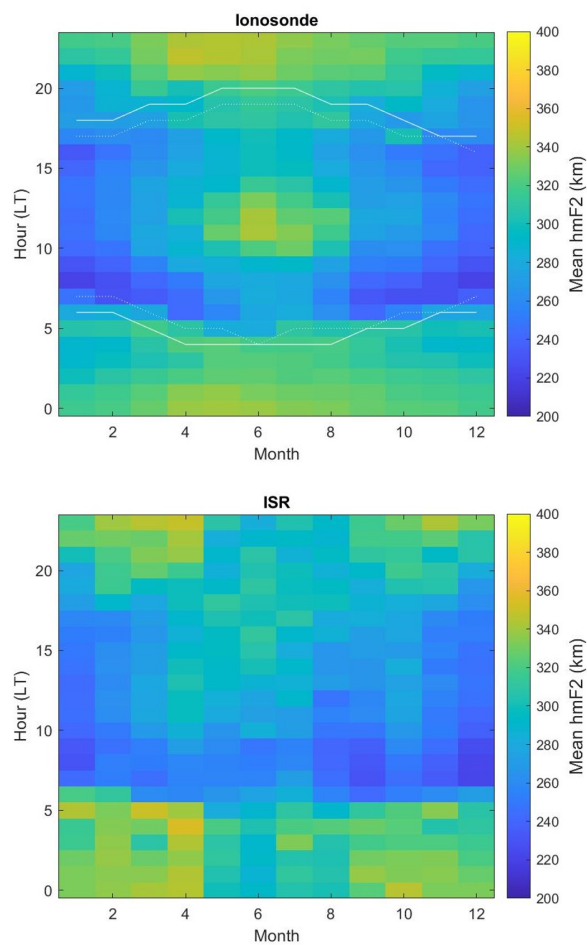


**Figure 3.** Monthly and hourly  $hmF2$  values averaged over the 35 years of common data (1986-2020) used in this study. Both ionosonde (top) and ISR (lower) derived  $hmF2$  values show clear seasonal and diurnal variations, with higher  $hmF2$  values at night.

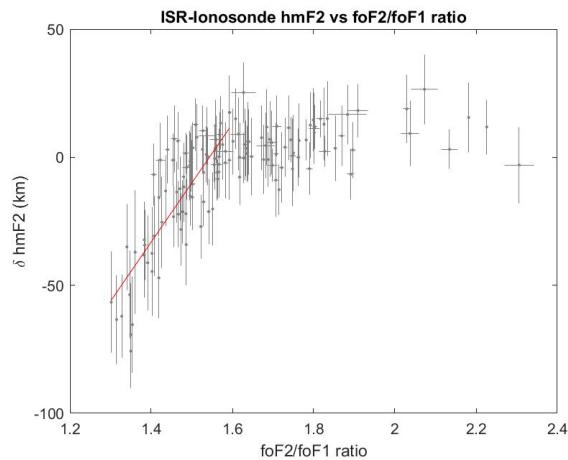


**Figure 4.** The difference between the ISR and ionosonde distributions shown in figure 3 plotted against the  $foF2/foF1$  ratio (for hours and months where such values exist). There is no significant difference between the two distributions for values of the  $foF2/foF1$  ratio above 1.6 but below this ratio, the presence of an  $foF1$  layer significantly affects the ionosonde-derived  $hmF2$  values due to the presence of underlying ionisation that is unaccounted for in the empirical formula. The red line represents a fit to the values corresponding to an  $foF2/foF1$  ratio below 1.6 (gradient  $231 \pm 21$ , offset  $-356 \pm 31 km$ )

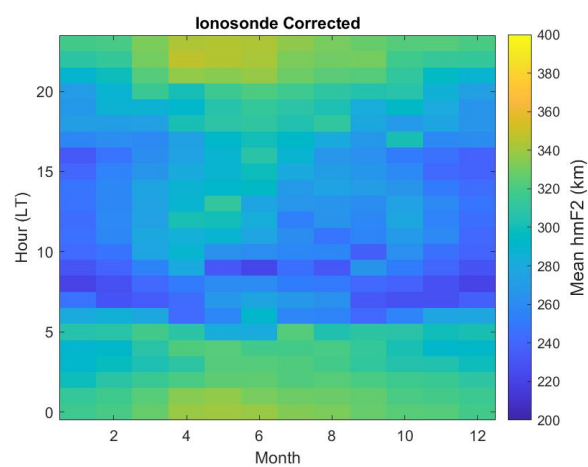


**Figure 5.** The same as for the top panel of figure 3 but with correction applied for bins where  $foF2/foF1 \leq 1.6$ . This has brought the summer daytime hmF2 values into closer agreement with those observed by the ISR (figure 5 lower panel

).

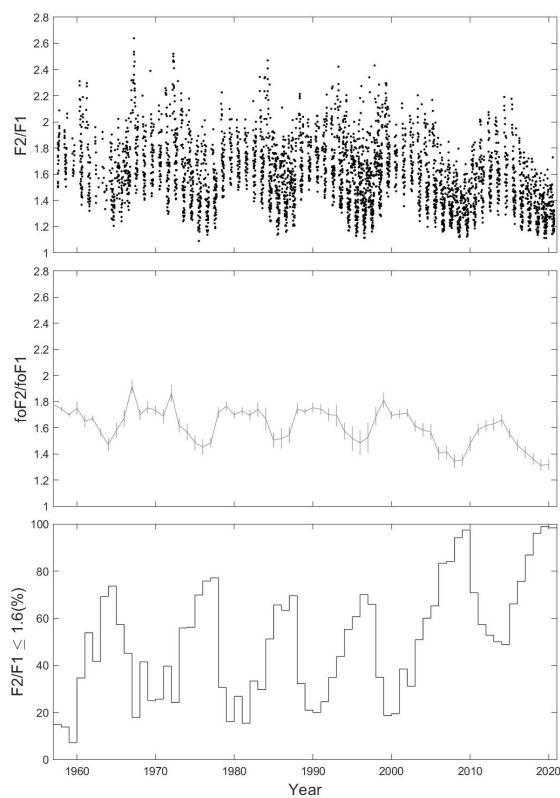


**Figure 6.** The foF2/foF1 ratio against year for hourly monthly median values (top panel), annual averages (middle panel) and the percentage of observations where foF1 is present for which the ratio is  $\leq 1.6$  (as identified in 4). It can be seen that there is a strong solar cycle dependence in this ratio, together with longer-term changes, particularly the apparent step change since the year 2000.

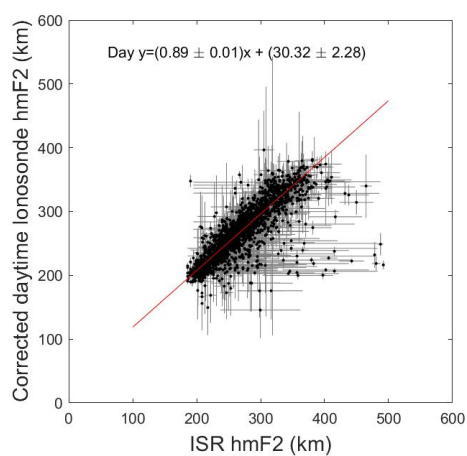


**Figure 7.** Hourly monthly median ionosonde-derived  $hmF2$  values, corrected for the presence of  $f_oF1$ , plotted against monthly mean  $hmF2$  values determined from the ISR, the correction results in a revised gradient of  $0.89 \pm 0.01$  with an offset of  $30.32 \pm 2.28 km$  (given by the red line).

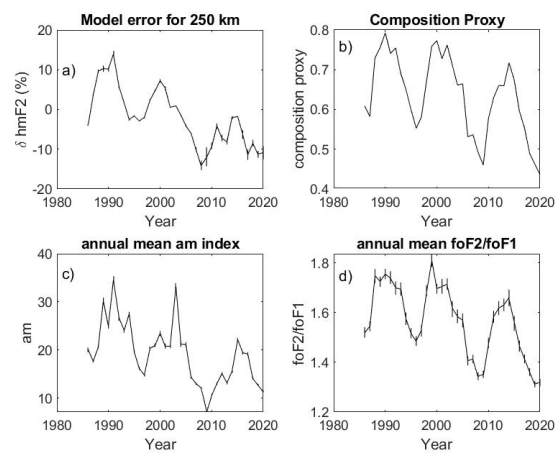


**Figure 8.** a) Percentage error in the empirical  $hmF2$  model after calibration with ISR data for each year in the range 1986-2020. b) Qualitative composition proxy based on annual average noon  $foF2$  value scaled by solar  $f10.7cm$  flux. c) Annual average values of the am index or the same epoch. d) The annual average ratio in  $foF2/foF1$  for the same epoch.

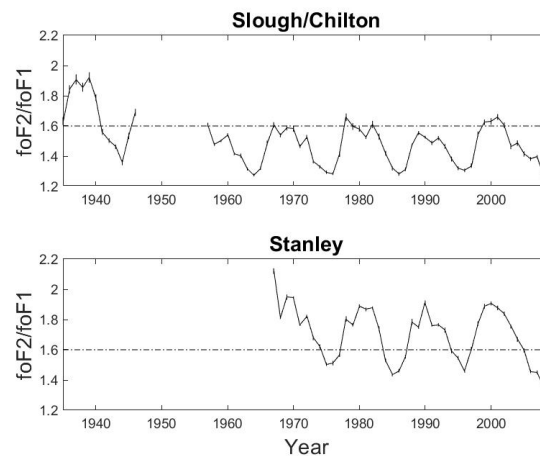


**Figure 9.** Annual mean  $foF2 : foF1$  ratio calculated from monthly hourly median data for two stations Slough/Chilton in the UK (top) and Stanley in the Falkland Islands (bottom). A ratio less than 1.6 has been shown to introduce bias into the empirical formula used to calculate  $hmF2$  from ionosonde data. The ratio remains below 1.6 for most of the data in the Slough sequence, making it far more sensitive to bias in  $hmF2$  calculations than Stanley, where the ratio is above 1.6 for a far greater proportion of the data. This will result in regional bias in observed  $hmF2$  trends.